Linear transduction of natural stimuli by dark-adapted and light-adapted rods of the salamander, *Ambystoma tigrinum*

Tania Q. Vu*, Sean T. McCarthy † and W. Geoffrey Owen*†‡

**Graduate Group in Vision Science and † Department of Molecular and Cell Biology, Neurobiology Division, University of California, Berkeley, CA, USA*

1. We examined signal, noise and response properties of salamander rod photoreceptors by measuring: (a) the circulating current of rods which were adapted to darkness and to a wide range of backgrounds; (b) contrasts of natural environments; (c) the effect of adaptation on the linear response range of rods; and (d) the behaviour of rods responding to dynamically modulated stimuli having a range of contrasts found in nature.

2. In the dark, the circulating current contained two noise components analogous to those described in toad. A discrete noise component consisted of events occurring at a rate of 1 event per 32 s (21 °C) and had a variance of 0·036 pA^2. A continuous noise component contributed 0·022 pA^2 to the dark current, roughly equal to the discrete noise variance.

3. Exposure to a wide range of steady backgrounds (suppressing up to 80% of the circulating current), elicited a sustained fluctuating photocurrent having a power spectrum which resembled those of single photon responses and was consistent with the linear summation of single photon events; this indicates that the primary source of noise in the current is caused by the light.

4. Eighty-nine per cent of the contrasts (C) measured in natural environments had $|C| < 50\%$, where $C = |I - I_{mean}| / |I_{mean}|$. The linear response range elicited by brief flashes expanded with brighter backgrounds, well-encompassing flash contrasts of 100%.

5. Dynamically modulated stimuli and incremental flashes having contrasts similar to those in natural scenes elicited small currents which deviated by a few picoamps about the mean and the transfer functions computed from each type of stimulus–response pair closely corresponded to one another. These results indicate that in natural environments, rods behave as linear small-signal transducers of light.

All the information an animal can possess about its visual environment is represented as a spatiotemporal array of photocurrents in the outer segments of photoreceptors. To create a reliable perception of the environment, this representation must be interpreted with minimal uncertainty in real time. The ability to do this is necessarily limited by noise generated within the photoreceptor and by noise intrinsic to the light that it absorbs. In absolute darkness, the circulating current of the rod fluctuates randomly due to thermal isomerizations of rhodopsin and to thermal variations in the rate of hydrolysis of cGMP (Baylor, Matthews, & Yau, 1980; Rieke & Baylor, 1996). In the presence of background illumination, additional fluctuations reflect the Poisson variability of photon absorption. Due to this noise, the distribution of photocurrents can never provide more than an uncertain representation of the visual world. Yet in spite of this, it is clear that the visual perception of many animals is highly reliable. To understand how such reliability is achieved, we must understand both the nature and sources of noise and the nature of the visual signals that the animal must process.

In this paper we describe experiments in which we quantify the noise in the circulating currents of salamander rods both in darkness and in the presence of a wide range of background intensities spanning the normal operating range of the rods. We show that, in the presence of background illumination, the Poisson variability of photon absorptions constitutes the dominant source of current noise. By comparing the power spectra of the measured noise with the power spectra of current responses measured under the same conditions, we also show that over a wide range of intensities, the steady-state photocurrent elicited by background illumination is a linear sum of single-photon responses. We measured the range of contrasts in a variety of natural environments and found that when stimulated with light modulated over a similar range of contrasts, the

‡ To whom correspondence should be addressed at 181 Life Sciences Addition, University of California, Berkeley, CA 94720-3200, USA.

response of the rod is a linear transformation of the stimulus. We conclude that under normal conditions, in a natural environment, rods behave as linear transducers of light.

METHODS

Animals and solutions

Experiments were performed on rod photoreceptors isolated mechanically from the retina of the larval tiger salamander (*Ambystoma tigrinum*). All procedures were carried out in accordance with guidelines approved by the Animal Care and Use Committee of the University of California at Berkeley and conformed to the recommendations of the NIH Guide for the Use of laboratory Animals (Publication no. 85-23), the ARVO Statement on the Use of Animals in Ophthalmic and Visual Research, and the USA Animal Welfare Act.

Larval tiger salamanders were kept in a tank containing aquarium plants, rocks, gravel and freely running water. Room temperature was maintained at 7 °C and room illumination was set on a 12 h dark–12 h light cycle.

Salamanders were dark adapted for 12–18 h prior to an experiment. At the start of an experiment, a salamander was stunned and quickly decapitated and pithed in dim red light. Under a microscope equipped with an infra-red converter, both eyes were removed and placed in salamander Ringer solution-filled vials. One eye was placed on filter paper, the anterior half of the globe was removed, and the remaining eyecup was transferred to a small pool of Ringer solution in a Sylgard-lined Petri dish. The retina was separated from the eyecup, oriented photoreceptor-side up, and halved with a razor blade. Rods were then mechanically isolated by chopping each half-retina several times with a razor blade. Rod suspension (200 μl) was pipetted into a Ringer solution-filled recording chamber mounted on the stage of an inverting microscope inside a light-proof Faraday cage in a dark room. The second eye was then hemisected and the eyecup was stored in a Ringer solution-filled light-tight vial on ice for later use (< 5 h).

The salamander Ringer solution contained (mM): 94 NaCl, 27 $NaHCO_3$, 3·5 KCl, 0·6 $MgCl_2$, 0·6 $MgSO_4$, 1·5 $CaCl_2$, 1 ascorbic acid, 3 Hepes, 9 glucose and buffered to a pH of 7·55 with *N*-methyl-D-glucamine.

The temperature of the Ringer solution in the recording chamber, measured with an immersion probe thermometer (Fluke 51, John Fluke Inc., Everett, WA, USA), remained constant during the course of a single experiment, and ranged from 20–21 °C between day-to-day experiments.

Stimulation and recording

Two narrowband green light emitting diodes (LEDs; AND180PGP, AND Inc., Burlingame, CA, USA; λ_{peak} 567 nm) provided the light for a dual beam optical system which focused two concentric circular spots (120 and 135 μm diameter) onto the plane of the chamber floor. An infrared LED (λ_{peak} 890 nm) was used to monitor and position rods in the recording electrode but was turned off during all recordings. Stray light was minimized by enclosing the optics in a covered box and the preparation in a light-tight Faraday cage. Light measurements indicate that the dim red light in the room during experiments would produce a maximum of 1/377 Rh* s^{-1} in a rod. Dark-adapted current recordings were performed in total darkness.

LED intensities were set by a computer-controlled current source and a combination of neutral density filters which provided additional light attenuation. Light calibrations were performed using two light meters (United Detector 351 (Graseby Optronics, Orlando, FL, USA) and IL1700 (International Light, Newburyport, MA, USA)), each equipped with independently calibrated silicon-sensor heads. A collecting area of 18 μm^2 was determined from mean rod dimensions and the optical density of rhodopsin at the peak of the stimulus wavelength (Harosi, 1975). Rods themselves were used to check light calibrations by using the linear relation between flash intensity and mean dim flash response, and by counting photon responses during dim background illumination.

For experiments during which rods were exposed to dynamically modulated backgrounds, the computer-controlled current source drove a green LED (at a digital update rate of 100 Hz, well above the frequency response of the rod) with a time course whose waveform had a white or $1/\omega^2$ power spectrum. (The white-noise stimulus was pseudorandomly generated from a Gaussian distribution using a MATLAB statistical toolbox algorithm. The amplitude spectrum of the white-noise stimulus was flat up to the Nyquist frequency and the amplitude spectrum of the $1/\omega^2$ stimulus had a logarithmic slope of minus one.) The response of the LED was confirmed by the correspondence of the time course of the LED light intensity, measured using a light sensor (United Detector 262), and the current waveform driving the LED. In the course of the experiments using these dynamic light stimuli, a rod was adapted to the mean background of the $1/\omega^2$ or white-noise stimulus for at least 35 s, then presented with ten alternating trials of each stimulus. The contrast of the dynamically modulated light stimulus was computed as the S.D./mean over its 10 s duration.

The rod current was recorded with a suction pipette and amplified by a virtual ground current-to-voltage converter (Baylor *et al.* 1979*a*). Suction electrodes were fashioned with i.d. ~10 μm and o.d. ~40 μm. An electrode containing a cell typically had a resistance of 4·5–9·0 MΩ. From this we calculated that 75–80% of the photocurrent was recorded.

Over long recording sessions, it was necessary to ensure that the cell would not move in the electrode. Generally, before any data were obtained, stability was checked by letting the newly suctioned cell sit in the electrode for 20–30 mins; after this period, if the recordings still contained obvious linear drift, the cell was rejected. With this protocol, it was usually unnecessary to adjust the position of the cell during the entire recording session.

For experiments during which rods were exposed to long-duration backgrounds, care was taken to ensure that the cell had returned to its dark-adapted state between responses by monitoring flash sensitivity with brief control flashes. Saturating response amplitudes were carefully monitored over the course of the experiment.

The current was filtered with an 8-pole Butterworth low-pass filter (Krohn–Hite model 3750, Avon, MA, USA) at a cut-off frequency of 15 Hz, sampled at 40 Hz (during dark and adapting-background experiments), and sampled at 50 Hz (during dynamically modulated background experiments).

Spectral analysis

The power spectrum of the photocurrent was used to isolate and characterize current noise in rods. The power spectrum of a waveform describes its variance distribution as a function of frequency. The one-sided power spectrum is defined as:

$$S(f) = 2E\left[\frac{|X(f)|^2}{T}\right], \quad (1)$$

where $X(f)$ is the Fourier transform of the current trace, T is the duration of the current trace, and $E[\ ]$ is the mean periodogram

computed from samples of $|X(f)|^2$. Power spectrum estimates were made using a MATLAB algorithm which implements Welch's method of spectrum estimation (Welch, 1978). Current records were segmented, individually linear detrended, weighted with a Hanning window, and half-overlapped. The Fourier transform of each segment was computed and the mean periodogram produced the estimate of the power spectrum. For adapting background experiments, the power spectrum was computed from steady-state current records ($t > 30$ s after stimulus onset) which were partitioned into segments, each 25·6 s long (1024 points). For dark-adapted experiments, the power spectrum of noise components was computed from concatenated segments of the dark current (each 51·2 s long) which contained or excluded discrete noise events. Similarly, the power spectrum of the steady-state saturating responses was computed from current records which were partitioned into segments each either 25·6 s long (1024) or 51·2 s long (2048 points).

The power spectra of dim flash responses were obtained by computing the Fourier transform of the mean flash response and squaring its magnitude. Mean flash response records were zero-padded to extend the spectral frequency resolution (Bendat & Piersol, 1971).

Matched filtering

A matched filter was used to detect photon-like responses in dark current traces (Baylor *et al.* 1980). The matched-filtered dark current was obtained by convolving the dark current traces with a filter whose impulse response function was the time-reversed mean dim flash response. Visual counts of event occurrence in a cell were performed using matched-filtered current records obtained for lengthy recordings in any individual cell (6–33 mins); this ensured that more reliable estimates of event rate were made.

Incremental flash response curves

Dark-adapted and background-adapted linear-range flash responses were described using the independence expression (Baylor *et al.* 1979*a*):

$$r_I(t) = Is_f e^{-\alpha t}(1 - e^{-\alpha t})^{n-1}, \quad (2)$$

where I is the flash intensity, s_f is the flash sensitivity, and α and n were adjusted by eye for best fit to the mean flash.

The power spectrum corresponding to these independence curves were computed as:

$$S_I(f) = \frac{S_0}{\prod_{c=1}^{n}\left(c^2 + \left(\frac{2\pi f}{\alpha}\right)^2\right)}, \quad (3)$$

where S_0 is the zero-frequency asymptote.

Contrasts in nature

Light intensities in natural environments were measured using a light metre equipped with a probe which contained a silicon diode detector (approximately flat spectral sensitivity, United Detector 262) housed at the end of a light-tight cylinder lined with baffles. Two circular apertures (4 and 1 mm diameter), spaced 15·2 cm apart, were placed in front of the detector and limited the field of view of the detector. Simple geometry indicated that the bounding rays passing through both apertures would subtend an angle of 2 deg. Empirical measurements of the probe's aperture intensity profile, obtained by scanning the probe across an illuminated pinhole, indicated that the intensity profile had dropped to zero for angles subtending greater than 1 deg (0·5 deg from the principal axis). Our calculations show that the empirical measurements are consistent with the theoretical estimates given expectable variation in probe construction.

Measurements were taken in 10 different natural areas from mid to late afternoon (1–4 pm) in Tilden Regional Park (Berkeley, CA, USA) which is home to a variety of flora (woody and leafy groves, bushes, grasses), fauna (deer, newts, mountain lions, racoons), and types of terrain (lakeside landscapes, dry grassy hills, exposed soil and rock formations). In any one natural environment, the probe was mounted 1 m above the ground and aligned parallel to the horizon. Intensity samples were systematically measured by rotating the probe in a full circle and recording the light intensity at 15 deg intervals.

The contrast in a natural scene was computed as

$$C = |I - I_{mean}|/|I_{mean}|,$$

where I represents the intensity of one light sample and I_{mean} represents the mean of intensity samples spanning an angular distance about the point I. I_{mean} was computed by taking the mean of intensities which span $I-15$ deg to $I+15$ deg (the mean intensity computed over an angular distance of 30 deg) or by taking the mean intensity which lies between $I-45$ deg to $I+30$ deg (the mean intensity computed over an angular distance of 75 deg).

RESULTS

Intrinsic noise in dark-adapted current

Randomness in the current response of rods is distinguished here as extrinsic or intrinsic noise. Extrinsic noise arises from stochastic sources which operate independently from the biological mechanisms within the rod, while intrinsic noise sources include the stochastic nature of these biological processes. Two types of intrinsic noise have been well-characterized by Baylor *et al.* (1980) in the dark-adapted current of toad rods, and are termed the 'discrete' and 'continuous' noise components. The random thermal activation of rhodopsin gives rise to discrete noise which appears in the form of brief suppressions that are indistinguishable from photon-evoked responses. Continuous noise arises from the random activation of phosphodiesterase from within the phototransduction cascade, producing persistent fluctuations in the dark current (Rieke & Baylor, 1996). In order to assess the extent of intrinsic noise in salamander rods, we recorded the circulating current of rods in total darkness.

Examples of current traces recorded in darkness from two cells are shown in Fig. 1*A*. The dark current fluctuates about a mean value with occasional larger discrete suppressions. Matched-filtered versions of the dark current are shown as the smooth traces above each current trace. A comparison of the time course of discrete events, the dim flash response, and the curve describing the dim flash response is made for one cell in Fig. 1*B* with plots of the spectrum of the discrete events, the spectrum of the mean dim flash response of the cell, and the spectrum of the function fitted to the mean dim flash response (see legend). The power spectrum of the discrete events was obtained by computing the power spectral difference of current records containing discrete events and current records excluding discrete events (Baylor *et al.* 1980). The correspondence between the three sets of

spectra indicates that the time course of individual events is similar to that of the dim flash response. This was confirmed in measurements on five cells.

The discrete-event rate, estimated from visual counts of the matched-filtered versions of the current (Fig. 1*A*, smooth traces), was $0{\cdot}031 \pm 0{\cdot}005\ s^{-1}$ (all results are given as means ± S.D. unless otherwise stated; 7 cells), corresponding to a mean of 1 event every 32 s. Since these events have a time course resembling that of the dim flash response and the event rate is well above the maximum rate expected from stray light-induced isomerizations, we conclude that this component of noise is caused by thermally initiated activation of rhodopsin molecules.

The underlying fluctuations in the dark current include a second biological noise component as well as extrinsic noise caused by the recording system. The biological component of noise is uncorrelated with the system noise and can be separated from it by taking the difference between the power spectrum of current traces lacking discrete events and that of current traces recorded in response to a saturating light (Baylor *et al.* 1980). This difference spectrum is shown in Fig. 1*C* (same cell as Fig. 1*B*). The continuous curve through the data in Fig. 1*C* is the same curve fitted to the dim flash response in Fig. 1*B* less two filter stages (see legend). The shape of the curve provides a satisfactory fit to the data using the same parameters as were used to fit the dim flash response in this cell, consistent with an origin of the continuous component of noise within the transduction cascade (Baylor *et al.* 1980).

The variance of each noise component, computed by integrating over the power spectrum, is $0{\cdot}036 \pm 0{\cdot}023\ pA^2$ (5 cells) for the discrete component and $0{\cdot}022 \pm 0{\cdot}018\ pA^2$ (5 cells) for the continuous component. These two noise components contribute about equally to the dark current.

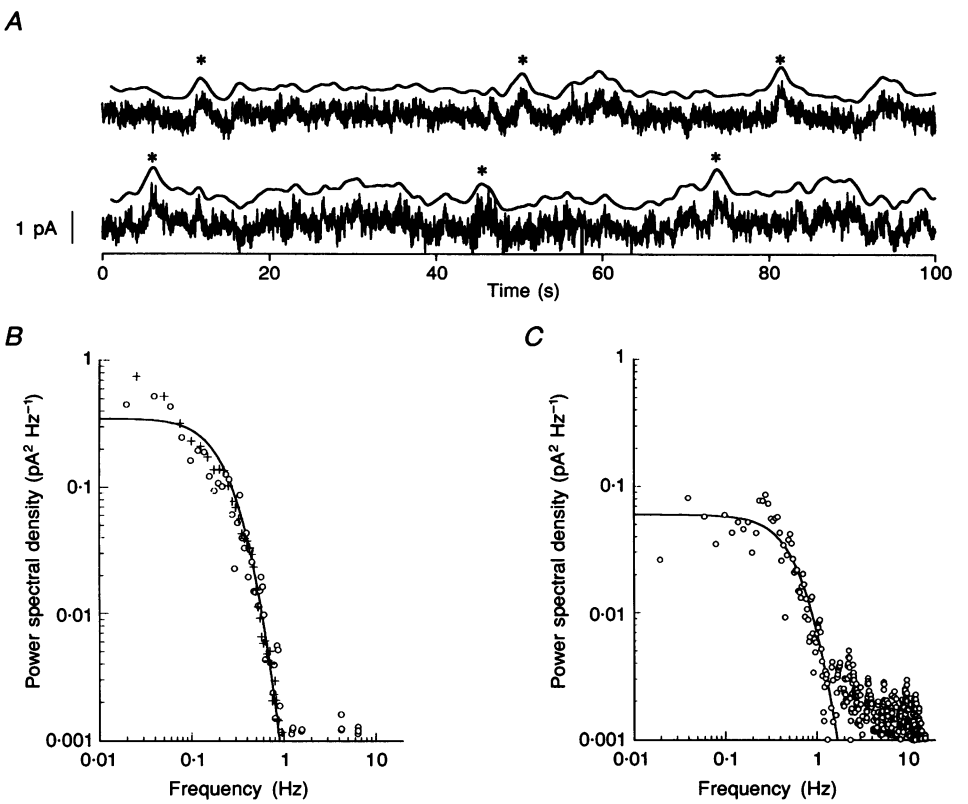

Figure 1. Components of noise in the dark current

A, current recorded in the dark (bold traces) from two different cells, low pass filtered at 15 Hz. Smooth curves above each trace are the matched filtered versions of the dark current below. * denote discrete responses. *B*, discrete component of noise. Comparison of: the power spectral difference of dark current records containing discrete events and excluding discrete events, taken from one cell (○); the power spectrum of the dim flash response in the same cell, positioned on *y*-axis by eye (+); and the power spectrum of the independence curve fitted to the dim flash response (smooth curve; eqn (3), α is 1·6; S_0 is 0·35; $n = 5$). *C*, continuous component of noise. Comparison of: the power spectral difference of dark current records excluding discrete events and the saturating current response (○), same cell as *B*; and the power spectrum of the independence curve fitted to the dim flash response of the same cell less two filter stages (smooth curve; eqn (3), c is 3; α at 1·6; S_0 at 0·06; $n = 5$). In *B* and *C*, each point (○) at $f > 1$ Hz, is a mean of 5 neighbouring points and smooth curves are positioned on the *y*-axis by eye. Bandwidth 0–15 Hz.

This is similar to earlier findings in toad rods (Baylor *et al.* 1980).

Noise in the background-adapted current

When a rod is adapted to steady background illumination, its steady-state photocurrent exhibits fluctuations whose magnitude and frequency content vary as a function of the background intensity (Fig. 2*A*). Baylor, Lamb & Yau (1979*b*) showed that the presence of dim to medium background intensities up to 5 photons μm^{-2} s^{-1}, in toad rods (equivalent to about 90 Rh* s^{-1} for salamander rods), elicits a photocurrent which is a linear sum of photon responses. In the experiments described below, we recorded from rods systematically adapted to backgrounds spanning most of the operating range of the rod and tested the hypothesis that the fluctuations observed in the steady-state photocurrent at each background represent the linear sum of random single photon responses.

Figure 2*A* shows a family of current traces recorded from a cell exposed to a series of backgrounds ranging from 0·36 to 439 Rh* s^{-1}. A background of 439 Rh* s^{-1} suppressed 65% of the circulating current in this cell. The top trace in Fig. 2*A* is the saturating current response recorded at the end of an experiment and provides a measure of system noise. Each photocurrent trace reaches a steady-state level within 30 s of stimulus onset. At dim background intensities, individual photon responses appear as random discrete peaks in the photocurrent. Increasing background intensities up to I_b of 28 Rh* s^{-1} causes the power of the steady-state current fluctuations to increase. However, further increase in the background intensity, causes the power in the fluctuations to diminish. This relationship is illustrated in Fig. 2*C*; the filled circles plot the steady-state current variance as a function of background intensity. In these experiments, linear range incremental flashes corresponding to each background were elicited from the same cell. Figure 2*B* (continuous traces) shows the mean flash responses elicited from the cell in Fig. 2*A* during exposure to each of these backgrounds. The incremental flash delivered, on average, 9 Rh* above the background intensity. The mean of the incremental flash responses corresponding to each background could be described by the independence equation (eqn (2)) and are shown in Fig. 2*B* as the dashed curves.

In Fig. 3*A* and *B*, the open symbols plot the power spectral difference of the background-adapted current and the saturating current for four of the background-adapted current traces in Fig. 2*A*. Each of these spectra resembles a

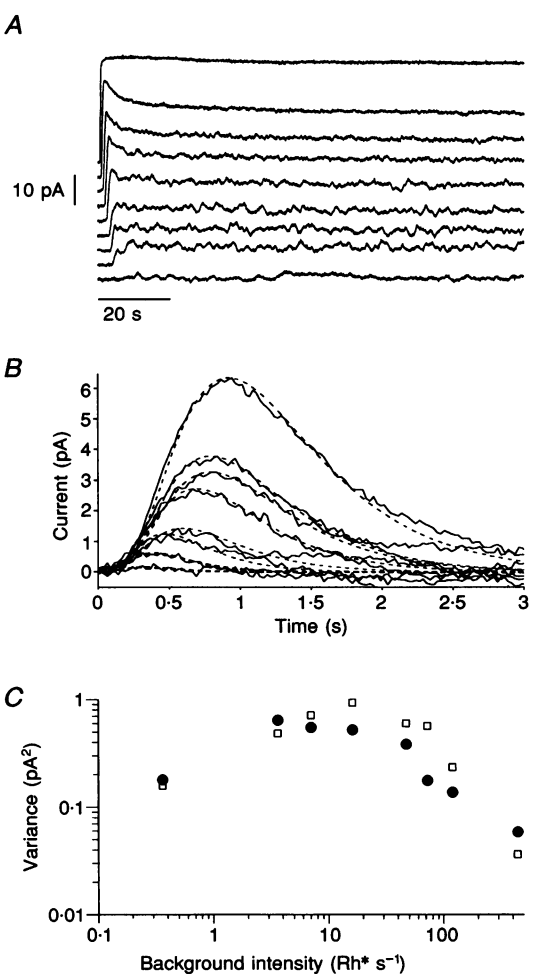

Figure 2. Background-adapted current responses, corresponding light-adapted flash responses, and plot of current variance as a function of mean background intensity

A, current traces recorded from a cell in response to a step of steady background illumination of (bottom to top): I_b = 0·36; 3·6; 7; 16; 47; 72; 119; 439 and 18 000 Rh* s^{-1}. Top trace is a bright background which completely suppresses the dark current and provides a measure of system noise. Current traces are offset on the *y*-axis at 5 pA intervals and positioned along the *x*-axis for display. *B*, continuous traces are means (n = 10) of light-adapted flash responses, (25 ms flash at t = 0 delivering 9 Rh*), corresponding to each of the adapting backgrounds in *A* (top to bottom: I_b = 0·36; 3·6; 7; 16; 47; 72; 119 and 439 Rh* s^{-1}). Dashed traces are the independence curve fit (eqn (2)) with parameters: n = 5; and (top to bottom) α = 1·8; 2·1; 2·1 ; 2·4 ; 2·8 ; 3·6 ; 4·4 and 5·4. Same cell as *A*. In *C*, ● is the variance of steady-state current in *A*, as a function of adapting background intensity; variance computed t > 30 s after stimulus onset; system noise subtracted. □ is the predicted current variance using eqn (5) (see later in Results: Current noise from single photon events).

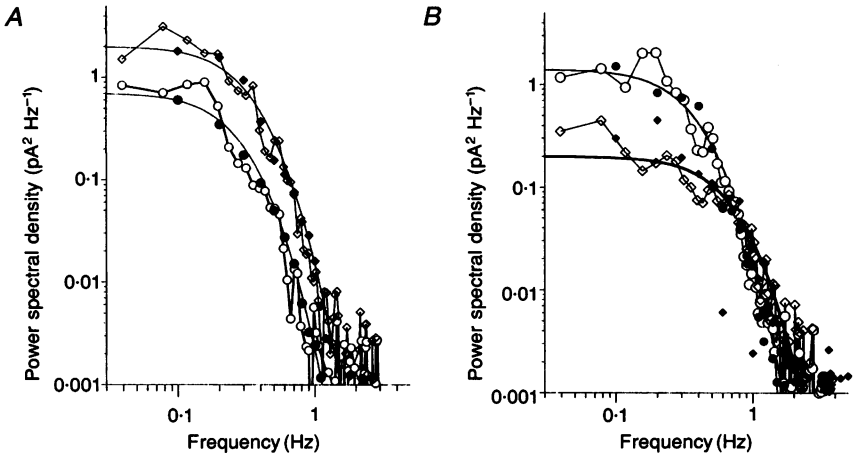

Figure 3. Comparison of power spectrum of current elicited by steady backgrounds and the light-adapted flash response

A, lower set of data (○, ●) correspond to $I_b = 0{\cdot}36$ Rh* s^{-1} and top set of data (◆, ◇) correspond to $I_b = 3{\cdot}6$ Rh* s^{-1}. ○ and ◇ are the power spectra of the steady-state background-adapted current, power spectrum of saturating response subtracted; ● and ◆ are the power spectrum of the mean adapted-flash response (positioned arbitrarily on *y*-axis). *B*, top set of data (○, ●) correspond to $I_b = 16$ Rh* s^{-1} and bottom set of data (◆, ◇) correspond to $I_b = 119$ Rh* s^{-1}. ○ and ◇ are the power spectra of the steady-state background-adapted current, power spectrum of saturating response subtracted; ● and ◆ are the power spectrum of the mean light-adapted flash response (positioned arbitrarily on *y*-axis). In *A* and *B*, each point (○, ◇) at $f > 3$ Hz, is the mean over 15 points. The continuous curves in *A* and *B* represent the power spectrum of the independence curve fitted to the corresponding incremental flash response, positioned arbitrarily on *y*-axis. Same cell as in Fig. 2.

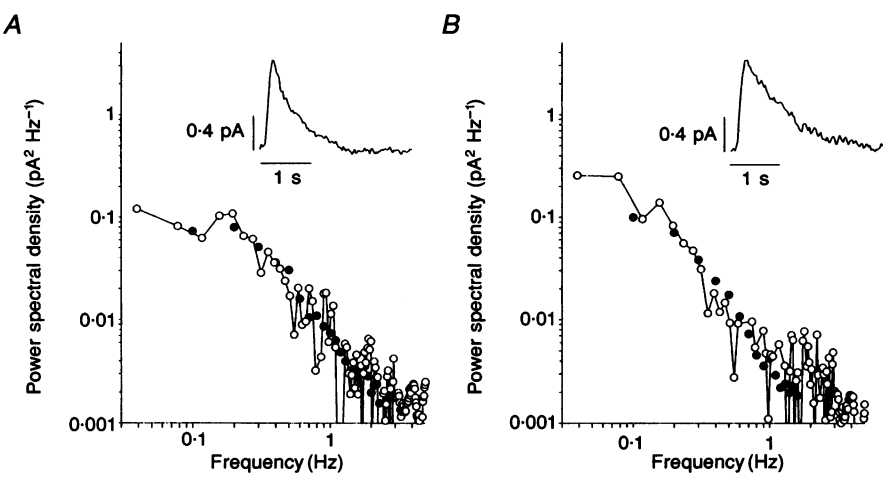

Figure 4. Comparison of power spectrum of current elicited by bright steady backgrounds and the light-adapted flash response for two cells

In *A*, ○ is the power spectrum of steady-state current response elicited by a steady background of $I_b = 951$ Rh* s^{-1}, 65% of the dark current suppressed, power spectrum of saturating response subtracted; ● is the power spectrum of the mean ($n = 15$) flash response (see inset) at the same adapting background, $I_b = 951$ Rh* s^{-1}. In *B*, ○ is the power spectrum of steady-state current response elicited by a steady background of $I_b = 951$ Rh* s^{-1}, 78% of the dark current suppressed, power spectrum of saturating response subtracted; ● is the power spectrum of the mean ($n = 15$) flash response (see inset) at the same adapting background, $I_b = 951$ Rh* s^{-1}. In *A* and *B*, ● is positioned arbitrarily on the *y*-axis and each point (○, ◇) at $f > 3$ Hz, is a mean over 15 points.

product of Lorentzian having a half-power point that shifts to higher frequencies with increasing background intensity. With an increase in background intensity from 0·36 to 3·6 Rh* s^{-1}, (Fig. 3*A*, open symbols), the DC asymptote of the spectrum shifts upwards on the vertical axis, but with an increase in intensity from 16 to 119 Rh* s^{-1}, (Fig. 3*B*, open symbols), the DC asymptote of the spectrum shifts downwards on the vertical axis.

Assuming that the fluctuations observed in each background-adapted current trace can be accounted for by the linear superposition of independent photon effects, the shape of the power spectrum for each background intensity should be similar to that of the linear incremental response elicited at that background (Fig. 2*B*). In Fig. 3*A* and *B*, the filled symbols are the power spectra of the incremental flashes (Fig. 2*B*) corresponding to the same adapting background. The smooth curves in Fig. 3*A* and *B* are the power spectra of the independence functions fitted to the linear range flash responses (eqn (3) in Methods). For each smooth curve, the parameters α and n correspond to those from the independence curve fits. The zero-frequency asymptote, S_0, was both adjusted by eye for best fit on the vertical axis and was computed from (Rice 1954):

$$S_0 = 2I_b[\int g(I_b,t)\mathrm{d}t]^2, \quad (4)$$

where I_b (Rh* s^{-1}) is the mean background intensity and $g(I_b,t)$ is the single photon response corresponding to I_b. Both methods yielded similar results; in Fig. 3 a comparison of S_0 as determined by best fit by eye and eqn (4) yielded respectively: 0·84 and 0·61 $pA^2\,Hz^{-1}$ for $I_b = 0{\cdot}36$ Rh* s^{-1}; 1·5 and 1·7 $pA^2\,Hz^{-1}$ for $I_b = 3{\cdot}6$ Rh* s^{-1}; 1·2 and 2·9 $pA^2\,Hz^{-1}$ for $I_b = 16$ Rh* s^{-1}; 0·35 and 0·31 $pA^2\,Hz^{-1}$ for $I_b = 119$ Rh* s^{-1}. The correspondence between the three spectra strongly support our hypothesis that the random fluctuations in the background current are accounted for by superposition of photon events. This was found to be true for all the backgrounds in Fig. 2*A*. A complete set of 7–9 adapting background current traces were recorded in each of three cells at background intensities ranging from 0·36 to 439 Rh* s^{-1} (suppressing up to 65% of the circulating current). Spectral analysis in these three cells produced similar results.

Even in the presence of brighter backgrounds, noise in the photocurrent appears to be primarily photon noise. This is shown in Fig. 4*A* for a cell which was adapted to a background intensity of 951 Rh* s^{-1} which suppressed 65% of the circulating current. A similar comparison is made in Fig. 4*B* for another cell; here a background of 951 Rh* s^{-1} suppressed 78% of the circulating current. The agreement between the spectrum of the adapted photocurrent and that of the incremental flash response was found in all of the six cells examined in the presence of bright adapting backgrounds which suppressed 65–78% of the circulating current.

Current noise from single photon events

During adaptation to background illumination, if the steady-state current response of the rod is a linear transformation of random photon arrivals, its exact time course cannot be predicted, but mean properties of the current such as power can be examined in either the time or frequency domain. Following Rice's development of Campbell's theorem for the output behaviour of a linear system whose input consists of Poisson-distributed random events (Rice 1954):

$$\sigma^2_{j(I_b,t)} = I_b\int g(I_b,t)^2\,\mathrm{d}t, \quad (5)$$

where I_b (Rh* s^{-1}) is the mean background intensity, $\sigma^2_{j(I_b,t)}$ (pA^2) is the variance of the steady-state photocurrent response to background I_b; and $g(I_b,t)$ is the single photon response corresponding to I_b.

The background intensity I_b can be computed by solving eqn (5) and using measured values of the remaining parameters: $\sigma^2_{j(I_b,t)}$ was computed directly from records of the adapted photocurrent, and $g(I_b,t)$ was obtained from the mean incremental flash response in the presence of the corresponding background. In Fig. 5, the predicted background intensities are plotted as a function of the measured background intensities; the data fall along the line which has a slope of unity. The variance $\sigma^2_{j(I_b,t)}$

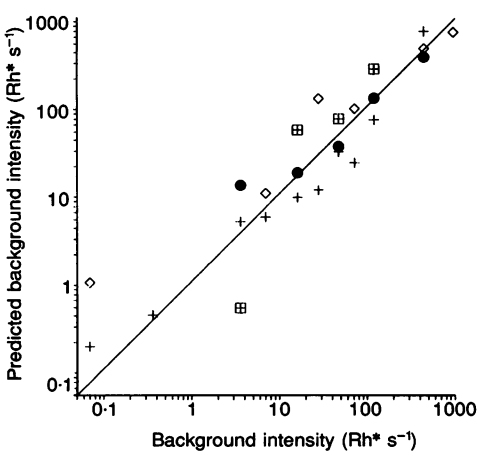

Figure 5. Comparison between the predicted and measured background intensity

The slope of the line is unity. The differing symbols represent four different cells. Predicted background intensity based on superposition of individual photon events (see text and eqn (5)).

computed from eqn (5) is compared with the measured variance in Fig. 2*C* (open squares).

Taken together, these results indicate that (1) a rod, adapted to background intensities within almost all of the normal operating range of the rod, acts as a linear transducer of photon absorptions and (2) extrinsic photon noise, an inseparable component of all luminous stimuli, is the predominant source of uncertainty in the rod photocurrent.

Rod signalling of dynamic contrasts present in natural environments

For a rod which is exposed to a steady background, the number of photons that arrive at its outer segment in a short time interval varies about the mean background rate with a Poisson probability. This randomness in photon arrivals constitutes a perturbation about a mean photon rate which lies within the linear range of operation of the rod (current fluctuations reflect the linear summation of random photon arrivals); the randomness of light means that a steady background of 16 Rh* s^{-1} would have a contrast of 25% (S.D./mean), whereas a background of 100 Rh* s^{-1} would have a contrast of 10%. In natural environments, it is likely that contrasts are limited, (Laughlin, 1981; Shapley & Enroth-Cugell, 1984), since the reflectances of natural objects fall within a narrow range (Krinov, 1953), and ambient light levels, as governed by the solar and/or lunar cycle, do not change rapidly. In this section we test the hypothesis that the contrasts a rod typically experiences in a natural scene are low and do not range widely above the contrasts set by photon fluctuations, thus implying that the rod photocurrent is a linear transformation of photon absorptions. Below, we describe light measurements made to assess the range of contrasts in natural environments, evaluate the linear response range of the rod using brief incremental flashes having contrasts limited by natural scenes, and directly test response linearity by exposing rods to dynamically modulated light stimuli whose contrasts were similar to those in natural environments.

Contrasts in natural environments. Light intensity measurements were performed in ten diverse natural environments using a narrow-field light sensor (see Methods). Light intensity samples in any one natural area were measured at angular intervals of 15 deg in the horizontal meridian. Although there was a diverse mix of

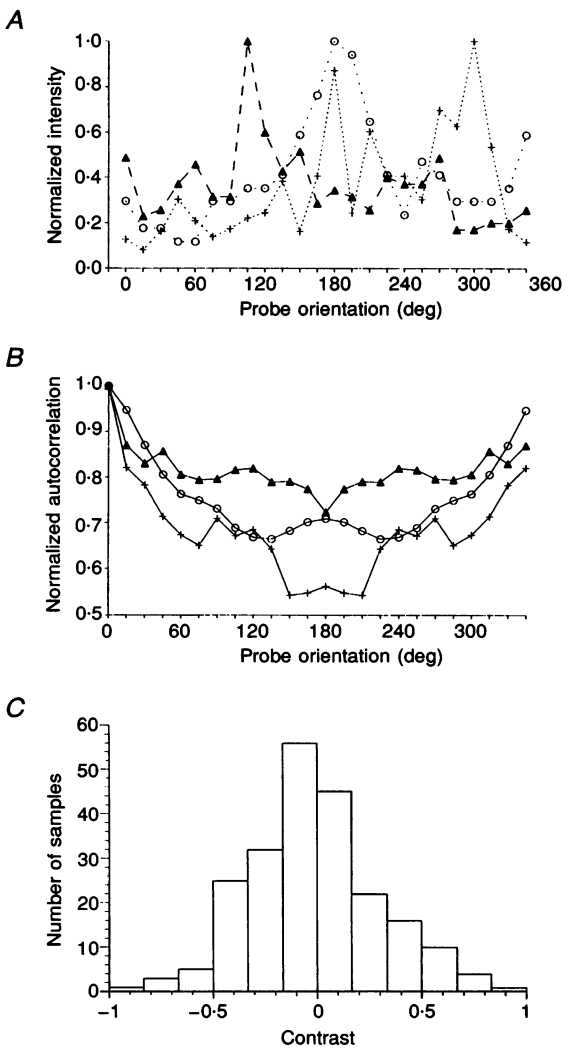

Figure 6. Intensities measured in a variety of natural areas using a narrow-field light sensor

A, sample intensity profiles measured in three natural areas: in a eucalyptus grove (+), on a bare soil path surrounded by leafy vegetation from trees and shrubs (△) and on an exposed lakeside rock formation (○). Profile intensities are normalized by the maximum intensity of the samples in each natural area. *B*, normalized autocorrelation of the intensity profiles in *A*. *C*, histogram of contrasts computed from 220 measured light samples. Contrasts computed as $C = (I - I_{mean})/I_{mean}$; I_{mean} computed over a angular span of 30 deg (see Methods). 89% of the samples have $|C| < 50\%$ and 60% of the samples have $|C| < 25\%$.

terrain, vegetation, and sunlit/shady interfaces among the different natural areas, the intensity profiles from each area did not markedly differ. Figure 6*A* shows the intensity profiles recorded from three different natural areas (see legend). As one might expect, intensity values over a range of small angular intervals were similar but started to deviate from one another over larger angular intervals. This is also illustrated in Fig. 6*B* which shows the autocorrelation function computed for each intensity profile in Fig. 6*A*.

The contrast histogram in Fig. 6*C* was constructed from 220 measurements of light intensities obtained in these ten natural areas. Eighty-nine per cent of the intensity samples had contrasts $|C| < 50\%$; over half of the samples (60%) had $|C| < 25\%$. The contrasts were computed using an angular span of 30 deg for I_{mean} (see Methods). One might perhaps expect that an I_{mean}, computed using a wider span than 30 deg, would yield a wider dispersion of contrast values and a less peaked histogram distribution. The autocorrelation functions (Fig. 6*B*) reveal a drop in correlation at 75 deg, relative to that at 30 deg. However, the histogram distribution of contrast values computed using a span of 75 deg for I_{mean} was very similar to that shown in Fig. 6*C*; 80% of the contrast values had a $|C| < 50\%$. These results set a physiologically relevant range of light levels for a rod viewing a natural scene.

Extent of the linear range of the rod. To assess how rods respond to the range of contrasts found in natural scenes, we recorded responses to brief (25 ms) flashes from rods that were adapted to a range of steady adapting backgrounds. It is a general property of vertebrate photoreceptors that when adapted to background illumination, vertebrate rod responses to brief flashes scale linearly in shape and amplitude over a range of incremental flash intensities. Figure 7*A* is a plot of the peak amplitude of the mean flash response as a function of flash intensity, for different adapting backgrounds. Associated with each background is a range of incremental flashes which elicit linear current responses. The peak amplitudes of the linear range responses lie on a line which passes through the origin and whose slope has the value of the flash sensitivity. This is illustrated by the dotted lines which correspond to the background intensities: $I_b = 3{\cdot}6$, 47, and 439 Rh* s^{-1}; the slope of each line is the ratio of the peak response amplitude elicited by the dimmest incremental flash at each background (6 or 10 Rh* s^{-1}) and the incremental flash intensity. The time course of the incremental flash responses were also examined to check for scaling in shape as well as amplitude. For example, Fig. 7*B* contains three incremental flash responses elicited by 6, 10 and 20 Rh* for an adapting background of 3·6 Rh* s^{-1}. Each flash response has been divided by the value of each corresponding flash intensity.

Figure 7*A* illustrates that with an increase in mean adapting background intensity, the flash sensitivity drops (described by Weber's law) and the range of flash intensities, which evoke linear responses, expands. The intensity of a flash which deviates from the intensity of the mean

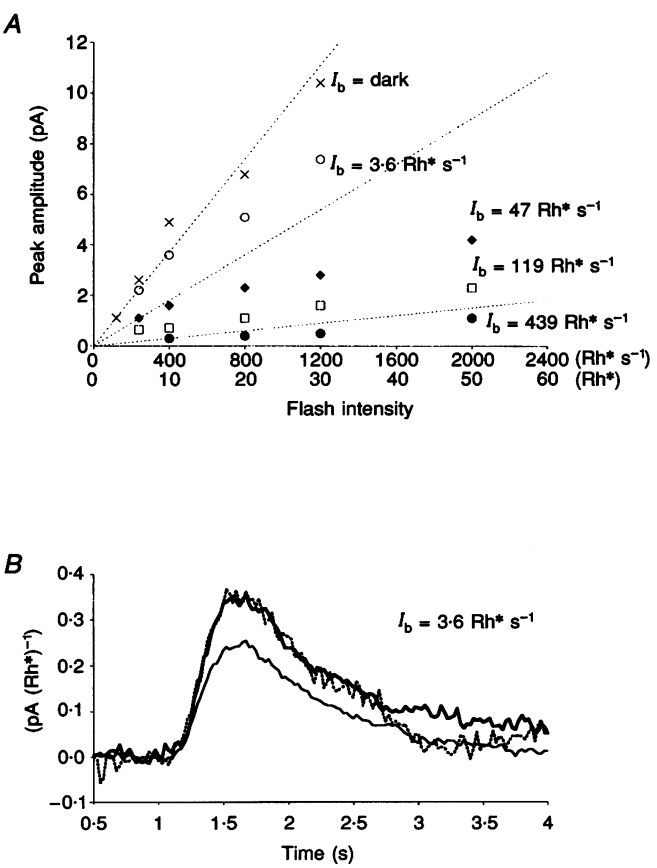

Figure 7. Linear range of light-adapted flash responses

A, graph of peak amplitude of light-adapted flash response as a function of flash intensity for one cell. Abscissa labels denote flash intensity in units of both Rh* s^{-1} and Rh*. Flash of 25 ms; flash responses are means of 15; symbols represent different adapting background intensities. Dotted lines correspond to I_b= 3·6, 47 and 439 Rh* s^{-1}; the slope of each line is the value of the flash sensitivity, determined from the lowest intensity flash response at each background (6 or 10 Rh*). *B*, plot of incremental flash responses corresponding to the first three points of background 3·6 Rh* s^{-1} in *A*: dotted line is the response to 6 Rh*, bold continuous line is 10 Rh*, and thin continuous line is 20 Rh*. Responses have been divided by the flash intensity.

background by one half (has a Weber contrast of 50%) is: 5·4 Rh* s^{-1} for $I_b = 3·6$ Rh* s^{-1}; 71 Rh* s^{-1} for $I_b = 47$ Rh* s^{-1}; 179 Rh* s^{-1} for $I_b = 119$ Rh* s^{-1}; and 659 Rh* s^{-1} for $I_b = 439$ Rh* s^{-1}. These flash intensities lie well within the linear range associated with each adapting background. In fact, the linear range at a background of 47 Rh* s^{-1} extends up to at least 400 Rh* s^{-1}. The actual limit of the linear range was difficult to determine at the brighter backgrounds (119 and 439 Rh* s^{-1}) since the small size of the flash responses is comparable to the system noise, but expansion of the linear range with increasingly brighter adapting backgrounds ensures that positive contrasts of at least 100% (an increment which is twice the mean background) will evoke linear incremental responses. The graph also illustrates that when adapted to a mean adapting background, contrasts of 100% evoke linear deviations in the photocurrent which are less than 1 pA in amplitude.

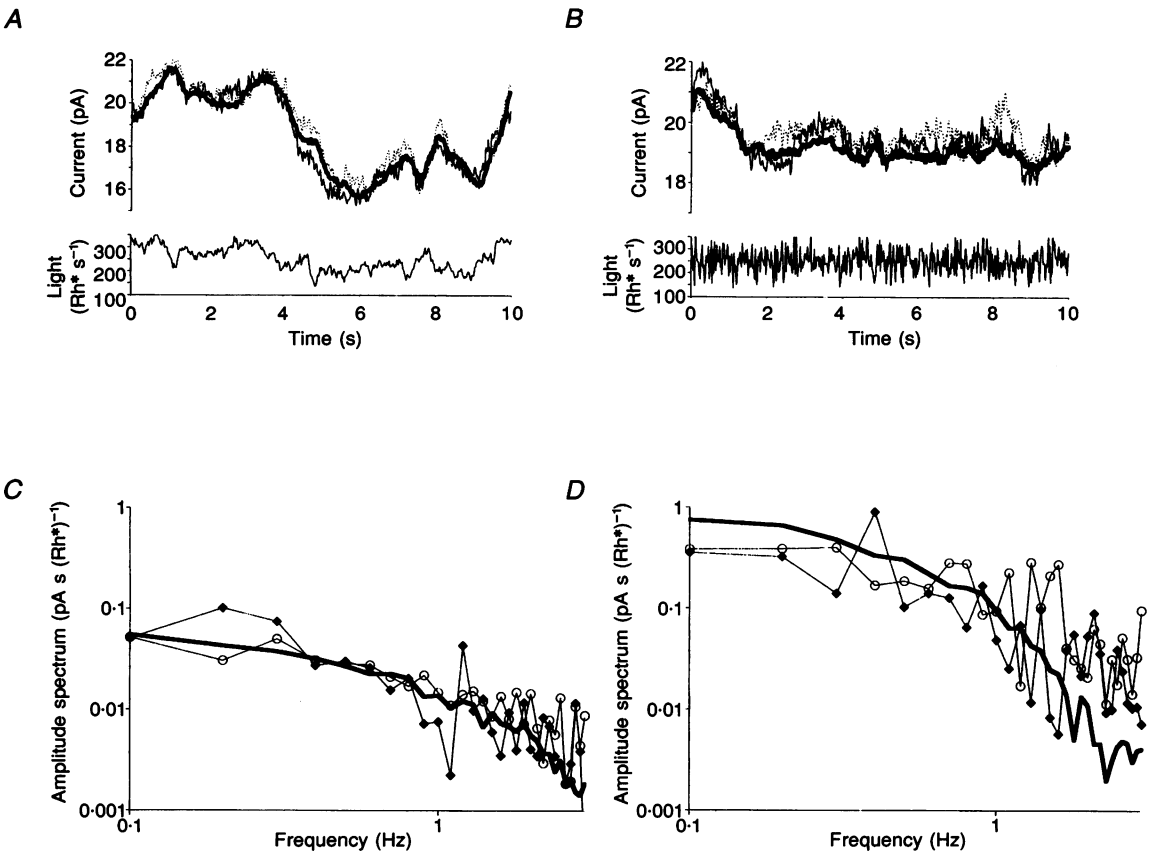

Figure 8. Amplitude spectrum of transfer functions for dynamically modulated $1/\omega^2$ stimuli, white noise stimuli and impulse response correspond closely in shape and magnitude

A, top plot is the current response (bold trace is the mean response, $n = 10$; light traces are individual responses) to a light stimulus (bottom plot). The light stimulus has a $1/\omega^2$ power spectrum, a contrast of 20% (S.D./mean) and a mean intensity of $I_b = 250$ Rh* s^{-1}. *B*, top plot is the current response (bold trace is the mean response, $n = 10$; light traces are individual responses) to a light stimulus (bottom plot). The light stimulus is Gaussian-modulated white noise with the same contrast and mean background as the light stimulus in *A*. *C*, comparison of the amplitude spectra of transfer functions computed from: mean $1/\omega^2$ stimulus–response pair shown in *A* (○); the white noise stimulus–response pair shown in *B* (◆); and the impulse response obtained from the incremental-flash response (bold continuous trace; 25 ms flash delivering 30 Rh*, mean flash response of $n = 36$). *D*, comparison of the amplitude spectrum of transfer functions computed from: the mean $1/\omega^2$ stimulus–response pair for a stimulus with contrast 65% and $I_b = 7·5$ Rh* s^{-1} (○); the white noise stimulus–response pair for a stimulus of contrast 65% and $I_b = 7·5$ Rh* s^{-1} (◆); and the impulse response obtained from the incremental flash response (bold continuous trace; 25 ms flash delivering 6 Rh*, mean flash response of $n = 36$). The current response in *A* and *B* has a delay of ~1 s relative to the light stimulus. Note that the white noise and $1/\omega^2$ stimuli were presented in alternating trials (see Methods); thus the start of each current record contains the delayed response to the stimulus presented in the previous trial. Transfer functions in *C* and *D* computed from the mean of 10 white noise stimulus–current pairs, and 10 $1/\omega^2$ stimulus–current pairs each over the 8 s interval (2 s into each stimulus–response trial).

Rod signalling of dynamically modulated light stimuli. In this section, we describe experiments during which we expose rods to dynamically modulated stimuli having contrasts similar to those measured in natural scenes and we test the hypothesis that in natural environments, photon absorptions are linearly transformed into the rod current waveform.

Analysis of natural scenes indicates that temporal variations in intensity follow a $1/\omega^2$ relation in the power spectrum (Dong & Atick, 1995). The top plot in Fig. 8*A* contains the current recorded (thick trace is the mean response, thinner traces are two raw responses) in response to a stimulus which had a $1/\omega^2$ power spectrum (bottom panel). This light stimulus had a contrast of 20% (S.D./mean) and a mean intensity, $I_b = 250$ Rh* s^{-1}. Note that the rod response to this stimulus deviates from the mean level by a few picoamps.

Band-limited white noise is frequently used to characterize systems because it is a rich stimulus, possessing power which is equally distributed over a range frequencies. Figure 8*B* contains the rod response (top plot) to a stimulus which was Gaussian white noise having the same contrast and mean background intensity as the stimulus in Fig. 8*A*. Again, the dynamically modulated stimulus elicits photocurrent deviations of a few picoamps about the mean. At a background of 7·5 Rh* s^{-1}, both a $1/\omega^2$ and white-noise stimulus with contrast 65% elicit photocurrent deviations of less than 3 pA in amplitude about the mean.

If, under these conditions, rods act as linear transducers, then the photocurrent will be a linear transformation of the light stimulus and the transfer function between the stimulus and photocurrent can be computed either from: (1) the ratio of the Fourier transform of the current response and the Fourier transform of the corresponding $1/\omega^2$ or white noise stimulus or (2) the Fourier transform of the impulse response. In Fig. 8*C* the circles are the amplitude spectrum for the ratio of the Fourier transform of mean response to the $1/\omega^2$ stimulus (from Fig. 8*A*) and a Fourier transform of the $1/\omega^2$ stimulus; the diamonds are the amplitude spectrum of the ratio of the Fourier transform of mean response to the white noise stimulus and Fourier transform of the white noise stimulus (from Fig. 8*B*); and the continuous curve is the Fourier transform of the impulse response elicited by a brief (25 ms) linear range incremental flash superimposed on the same mean adapting background ($I_b = 250$ Rh* s^{-1}). Figure 8*D* illustrates the same comparison for a higher contrast light stimulus (65% contrast) and a mean background, $I_b = 7{\cdot}5$ Rh* s^{-1}. In both plots, Fig. 8*C* and *D*, the three sets of data closely correspond both in magnitude and shape and are consistent with the hypothesis that the rod photocurrent is a linear transformation of dynamically modulated stimuli containing contrasts typical of natural environments.

DISCUSSION

Noise sources in the photocurrent

Over background intensities which span 2–80% of the operating range of the rod, the random fluctuations observed in the light-adapted current are accounted for primarily by the random (Poisson) nature of photon arrivals. Such noise is inseparable from the stimulus and is effectively an intrinsic part of the light signal. Intrinsic noise contributed by thermal activation of biological components within the cascade is ever present, but represents a significant fraction of the total noise power only during darkness and extremely dim backgrounds. Over the wide range of backgrounds tested (0·36–951 Rh* s^{-1}) the continuous component of the noise could not be distinguished in the power spectrum of the current. Likewise, the discrete component made a diminishing contribution to the total noise power with increasing background intensity. In the presence of a dim background of 0·36 Rh* s^{-1}, the discrete noise is equivalent to 0·031 Rh* s^{-1} and accounted for less than 8% of the total noise power. The primary source of noise at this and at all higher background intensities was the Poisson variability of photon absorption. Thus under most conditions, the primary source of uncertainty in interpreting the visual input is likely to be the quantal nature of the light itself.

Linear signalling of natural contrasts

The stimuli used to study the properties of retinal neurons – steps or flashes of light, spots or annuli – are chosen for a variety of reasons, usually because they offer some advantage to the investigator. What we can learn about stimulus–response properties such as linearity, variability, and fidelity, however, is determined to a large extent on the choice we make. The visual system has been shaped by evolutionary pressures and the importance of using natural stimuli in evaluating its performance is becoming increasingly clear, (Laughlin, 1981; Van Hateren, 1992; Dan, Atick & Reid, 1996 and S. T. McCarthy, T. Q. Vu & W. G. Owen, personal communication). We found that in a wide diversity of natural environments, the light intensities reflected by vegetation and terrain generally fall within a fairly narrow range about the mean intensity. An observer viewing a natural scene experiences mostly shallow modulations in intensity which deviate by less than 50% from the mean. These contrasts, typical of natural scenes, confer upon rods a functionally defined range of operation.

It has long been known that light-adapted rod responses are linear within a range of incremental flash intensities (Fain, 1976), and in response to small sinusoidal light modulations (Pinter, 1966). When we exposed rods to light stimuli whose time dependence and contrast were characteristic of natural scenes, we found them to respond linearly at all background intensities tested. We found that the intensity range of the linear response of a rod to a brief flash expands with increasing background intensities, well-encompassing responses to contrasts of 100%. Moreover,

our analysis of the spectral properties of the circulating current and of incremental flash responses, measured in the presence of background illumination whose intensities spanned most of the operating range of the rod, demonstrated that the steady-state response of the rod to steady light is a linear sum of the responses evoked by each of the photons it absorbs. Taken together, these results make clear that, in a natural environment, the rod can be expected to behave as a linear transducer. In recent work on the blowfly, light-adapted photoreceptors were found to respond linearly to temporally modulated white noise containing a wide range of contrasts, intended to simulate their visual environment during flight (Juusola, Kouvalainen, Jarvilehto & Weckstrom, 1994). Linear signalling of naturalistic light stimuli may thus be a general property of photoreceptors.

Small size of the current signal

The variations in the photocurrent elicited by a naturally modulated stimulus are small, deviating from the mean by no more than a few picoamps. This current is transformed into a voltage when it drops across the membrane impedance of the rod and it is this voltage which drives the synapse of the rod. Assuming a value of 600 MΩ for the membrane impedance of a solitary rod, (R. L. Miller & W. G. Owen, personal communication), we estimate the peak-to-peak variation in the voltage at the synapse of the rod evoked by any of the 'natural' stimuli we presented to have been no greater than 3 mV in amplitude. This implies that the salamander's perception of the visual world is based upon quite subtle changes in the presynaptic voltage and suggests that the rod synapse may be specialized for reliable signalling of such small deviations.

Baylor, D. A., Lamb, T. D. & Yau, K.-W. (1979*a*). The membrane current of single rod outer segments. *Journal of Physiology* **288**, 589–611.

Baylor, D. A., Lamb, T. D. & Yau, K.-W. (1979*b*). Responses of retinal rods to single photons. *Journal of Physiology* **288**, 613–634.

Baylor, D. A., Matthews, G. & Yau, K.-W. (1980). Two components of electrical dark noise in toad retinal rod outer segments. *Journal of Physiology* **309**, 591–621.

Bendat, J. S. & Piersol, A. G. (1971). *Random Data: Analysis and Measurement Procedures.* Wiley-Interscience, New York.

Bodoia, R. D., & Detwiler, P. B. (1984). Patch-clamp recordings of the light-sensitive dark noise in retinal rods from the lizard and frog. *Journal of Physiology* **367**, 183–216.

Dan, Y., Atick, J. J. & Reid, R. C. (1996). Efficient coding of natural scenes in the lateral geniculate nucleus: experimental test of a computational theory. *Journal of Neuroscience* **16**, 3351–3362.

Dong, D. W. & Atick, J. J. (1995). Statistics of natural time-varying images. *Network: Computation in Neural Systems* **6**, 345–358.

Fain, G. (1976). Sensitivity of toad rods: dependence on wave-length and background illumination. *Journal of Physiology* **261**, 71–101.

Gray, P. & Attwell, D. (1985). Kinetics of light-sensitive channels in vertebrate photoreceptors. *Proceeding of the Royal Society* B **223**, 379–388.

Harosi, F. I. (1975). Absorption spectra and linear dichroism of some amphibian photoreceptors. *Journal of General Physiology* **66**, 357–382.

Juusola, M., Kouvalainen, E., Jarvilehto, M. & Weckstrom, M. (1994). Contrast gain, signal-to-noise ratio, and linearity in light-adapted blowfly photoreceptors. *Journal of General Physiology* **104**, 593–621.

Krinov, E. L. (1953). *Spectral Reflectance Properties of Natural Formations.* Technical Translation TT-439 (Belkov, E., Translator); National Research Council of Canada: Ottawa.

Laughlin, S. (1981). A simple coding procedure enhances a neuron's information capacity. *Zeitschrift fur Naturforschung* **36C**, 910–912.

Matthews, G. (1986). Comparison of the light-sensitive and cyclic GMP-sensitive conductances of the rod photoreceptor: noise characteristics. *Journal of Neuroscience* **6**, 2521–2526.

Pinter, R. B. (1966). Sinusoidal and delta function responses of visual cells of the *Limulus* eye. *Journal of General Physiology* **49**, 565–593.

Rice, S. O. (1954). Mathematical analysis of noise. In *Selected Papers on Noise and Stochastic Processes*, ed. Wax, N., pp. 133–294. Dover, New York.

Rieke, F. & Baylor, D. A. (1996). Molecular origin of continuous dark noise in rod photoreceptors. *Biophysical Journal* **71**, 2553–2572.

Ruyter van Steveninck, R. R., Lewen, G. D., Strong, S. P., Koberle, R. & Bialek, W. (1997). Reproducability and variability in neural spike trains. *Science* **265**, 1805–1808.

Shapley, R. & Enroth-Cugell, C. (1984). Visual adaptation and retinal gain controls. *Progress in Retinal Research* **3**, 263–346.

Van Hateren, J. H. (1992). Theoretical predictions of spatiotemporal receptive fields of fly LMCs, and experimental validation. *Journal of Comparative Physiology* **171**, 157–170.

Welch, P. D. (1978). The Use of Fast Fourier Transform for the estimation of power spectra: a method based on time averaging over short modified periodograms. In *Modern Spectral Analysis*, ed. Childers, D., pp. 17–20. Wiley, New York.

Acknowledgements

We thank S. Ruffner and J. Nickel for careful reading and helpful comments on the manuscript. Funding for this study was provided by National Institute of Health Research Grant EY03785 to W. G. Owen.

Author's email address

W. G. Owen; gowen@uclink4.berkeley.edu

Received 13 May 1997; accepted 23 July 1997.